THE ASTROPHYSICAL JOURNAL, 454:463–471, 1995 November 20

NEW FEATURES OF THE X-RAY DIP SOURCE 1755−338

KWANG-IL SEON AND KYOUNG-WOOK MIN
Department of Physics, Korea Advanced Institute of Science and Technology, 373-1 Gusong-dong, Yusong-gu, Taejon 305-701, Korea; kiseon, kwmin@space.kaist.ac.kr

KENJI YOSHIDA
Kanagawa University, 3-27-1, Rokkakubashi, Kanagawa-ku, Yokohama 221, Japan; yoshida@xray.astro.isas.ac.jp

FUMIYOSHI MAKINO
Institute of Space and Aeronautical Science, 3-1-1, Yoshinodai, Sagamihara, Kanagawa 229, Japan; makino@xray.astro.isas.ac.jp

MICHIEL VAN DER KLIS AND JAN VAN PARADIJS
Astronomical Institute "Anton Pannekoek," University of Amsterdam and Center for High-Energy Astrophysics, Kruislaan 403, NL-1098 SJ Amsterdam, The Netherlands; michiel, jvp@astro.uva.nl

AND

WALTER H. G. LEWIN
Massachusetts Institute of Technology, Center for Space Research, Room 37-627, Cambridge, MA 02139; lewin@space.mit.edu

Received 1995 March 6; accepted 1995 May 31

ABSTRACT

The X-ray dip source 1755−338 was observed with *Ginga* and simultaneously with *Ginga* and *ROSAT* in 1991. The source was in the "high" luminosity state during the observation in 1990, similar to the *EXOSAT* observation. Regularly spaced dips and no apparent low-energy absorption during these dips are confirmed. During the observation in 1991, the source was in the "low" luminosity state with the flux (1–37 keV) less than 35% of the "high" state nondip level. The spectrum observed in this "low" state is much harder than that in the "high" state. Also, an iron emission line centered around 6.7 keV is found in the "low" state. The data imply that the accreting matter in this system might have the cosmic abundance, contrary to the earlier suggestion that the heavy-element abundances in 1755−338 are extremely low. The equivalent neutral hydrogen column density is $\sim 4 \times 10^{21}$ cm^{-2} in the low state, as deduced from the combined data of *ROSAT* and *Ginga*.

Subject headings: binaries: close — stars: individual (1755−338) — X-rays: stars

1. INTRODUCTION

About 10 low-mass X-ray binary systems (LMXBs) have been found to exhibit periodic dips in their X-ray intensity (Cominsky & Wood 1984; White & Mason 1985; Mason 1986, 1989; Parmar & White 1988; for a review see White, Nagase, & Parmar 1995). The recurrence period of the dips ranges from 0.19 hr (1820−303; Stella, Priedhorsky, & White 1987) to 235 hr (Cyg X-2; Vrtilek et al. 1986). These dips are often attributed to absorption and scattering in a "bulge" or thickened region of the outer accretion disk produced by the impact of the gas stream from the companion (White & Swank 1982). Eclipses are also seen in 1659−29 (Cominsky & Wood 1984) and in 0748−676 (Parmar et al. 1986).

Our subject 1755−338 is a bright source located in the general direction of the Galactic center. The distance to the source has been estimated to be less than 9 kpc (Mason, Parmar, & White 1985), and the X-ray luminosity is about 10^{36} ergs s^{-1} for an assumed distance of 3 kpc. The source has been optically identified with a 19th magnitude blue object with a featureless continuum (McClintock, Canizares, & Hiltner 1978; Bradt & McClintock 1983; van Paradijs 1995). Previous observations of 1755−338 have revealed several interesting features. The ultrasoft nature of the spectrum was noticed by Jones (1977) and confirmed subsequently by White & Marshall (1984), who showed that its location in the X-ray color-color diagram is shared with a number of black hole candidates. The *EXOSAT* observations showed the presence of recurrent dips with a 4.4 hr period; the spectrum during the dips did not show any apparent energy dependence, whereas most of the "dipping" sources show strong absorption in the low-energy X-ray region during the dips (White et al. 1984). The spectral independence of the 1755−338 dips led White et al. (1984) to suggest that the metallicity of the absorbing medium in the system might be at least a factor of 600 below cosmic values. Simultaneous *EXOSAT* and optical observations showed that the period of the optical modulation is consistent with the X-ray dip recurrence period, and the optical minimum occurred about 0.15 cycles after the center of the X-ray dip (Mason et al. 1985); this phasing fits the idea that X-ray dips are caused by the disk bulge, and that the optical light curve reflects the heating effect of the X-ray source on its companion star or an asymmetric disk.

The X-ray dip source 1755−338 was observed with *Ginga* in 1990 and simultaneously with *Ginga* and *ROSAT* in 1991. We report the results of these observations in this paper. In particular, we report the finding of the possible iron emission line when the intensity of the source was "low" in 1991. We also discuss the possibility that the compact object in the source is a black hole.

2. OBSERVATION AND ANALYSIS

The observations in the present study were made with the Large Area Counter (LAC) on board *Ginga* (Makino et al. 1987; Turner et al. 1989) in 1990 April and in 1991 September.

The observation in 1991 September was performed simultaneously with an observation with the Position Sensitive Proportional Counters (PSPCs) on board the *Röntgen Satellite* (*ROSAT*; Trümper 1983). The *Ginga* observations were carried out using the data modes MPC2 in 1990 April and MPC1 (Turner et al. 1989) in 1991 September. The background subtraction for the analysis of *Ginga* observations was done using the nearby sky data obtained one day before the observation in 1990 and those obtained 7 days after the observation in 1991. In the analysis of the *ROSAT* observations, only the Pulse Height Analyzer (PHA) channels 17 to 247, corresponding approximately to the energy interval from 0.17 keV to 2.5 keV for *ROSAT*, have been used. Background counts for the *ROSAT* observation were obtained from an annulus around the source, and the counts in the annulus were scaled to the area of the source aperture.

The light curves obtained from the first *Ginga* observations of 1755−338 in the 1–37 keV energy band are shown in Figure 1. The data of the first observation made between 1990 April 24, 07:24 (UT) and April 26, 05:40 (UT) are plotted in Figure 1*a*. The accumulation time of each bin is 60 s. As can be seen in the figure, there are many gaps in the data resulting from Earth occultation and passage of the South Atlantic Anomaly. Nevertheless, we can identify the low-intensity moments around April 24, 11 UT, 16 UT, 20 UT, April 25, 5 UT, 18 UT, 22 UT, and April 26, 3 UT, which we might call "dips" in view of the regular spacing as observed previously with *EXOSAT* (White et al. 1984). These dips are shallower than those seen with *EXOSAT*, the intensity in the dip center being more than 70%–80% of the unaffected intensity. The period of the dips in the present data is around 4.37 hr, not much different from the earlier estimation of 4.4 hr based on the *EXOSAT* observation. In addition to these primary dips, another small intensity drop with a central intensity of about 90% of the nondip level is seen just after April 25, 20 UT, halfway between the two primary dips seen around 18 UT and 22 UT. A light curve folded on the 4.37 hr period is shown in Figure 1*b*.

The data obtained during the second observation, performed with *Ginga* between 1991 September 22, 08:43 (UT) and September 23, 17:37 (UT), are plotted in Figure 2*a*, and their folded light curve on the same period (4.37 hr) as the first observation is shown in Figure 2*b*. The flux level is about 30%–35% of the nondip level observed in 1990. The folded light curve shows a very shallow minimum near 0.45 phase, corresponding to 1991 September 22, 11 UT, 19 UT, and 24 UT. The phase shift of the intensity minimum in Figure 2*b* relative to that of Figure 1*b* is not meaningful, since the interval of the two observations is so long that we cannot accurately determine the ephemeris with the known information about this source. The spectrum obtained from the 1991 observation

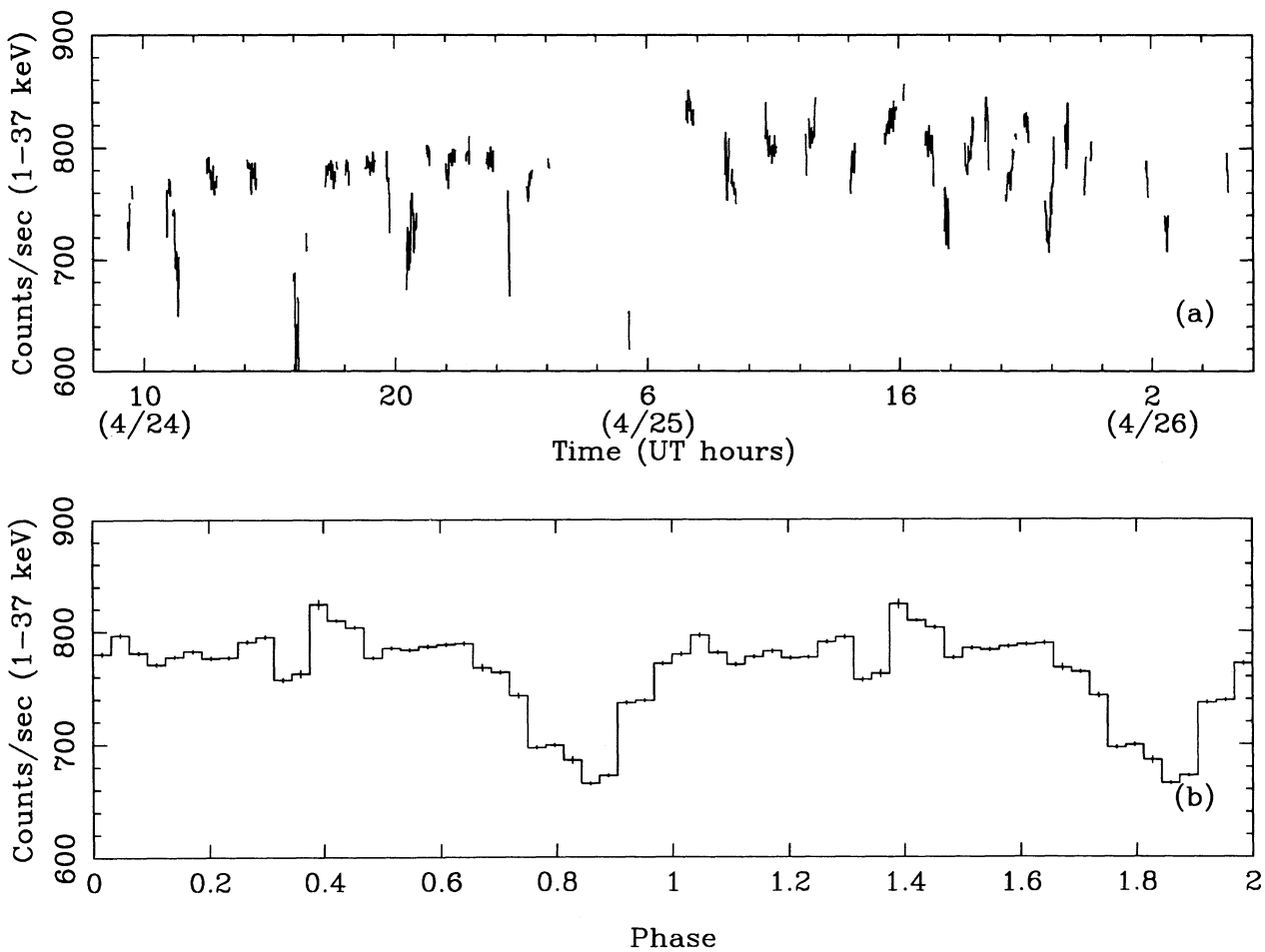

FIG. 1.—(*a*) *Ginga* LAC data of 1755−338 in the energy band 1–37 keV obtained from 1990 April 24–26. The time resolution is 60 s. (*b*) A folded light curve corresponding to (*a*) with the period 4.37 hr.

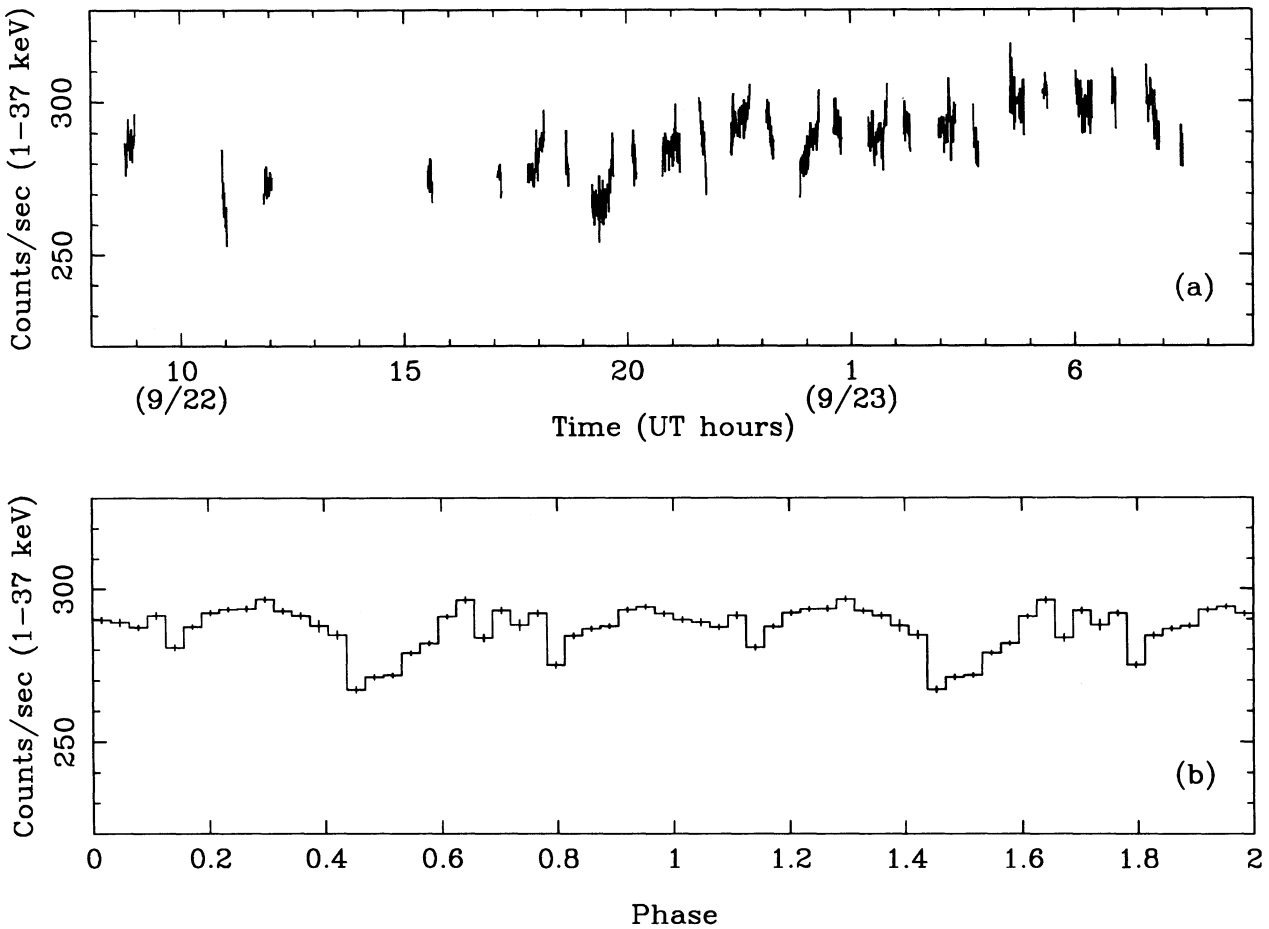

FIG. 2.—(*a*) *Ginga* LAC data of 1755−338 in the energy band 1–37 keV obtained in 1991 September. The time resolution is 32 s. (*b*) A folded light curve corresponding to (*a*) with the period 4.37 hr.

is very different from that of the 1990 observation, as shown in Figure 3, the hard tail being more prominent in this low-intensity state (hereafter, "low" state) compared to that of the high-intensity state in 1990 (hereafter, "high" state). *ROSAT* also performed a simultaneous observation in the soft X-ray range between 1991 September 22, 18:45 (UT) and September 23, 06:05 (UT). The count rate of *ROSAT* PSPC data in 1991 remains more or less constant at ~ 21 counts s^{-1}.

The spectra in the nondip and dip states of the 1990 observation are plotted in Figure 4. The luminosity of the nondip state is about 3×10^{36} ergs s^{-1} for an assumed distance of 3 kpc. Spectral fits to the nondip spectrum with simple single-component models are not successful. The best such fit is of the form $E^{-\alpha} \exp(-E/E_c)$, with $\alpha = 0.47 \pm 0.13$ and $E_c = 1.67 \pm 0.05$ keV, similar to the *EXOSAT* result (White et al. 1984). But the fit is rather poor, χ^2_ν being 2.25 for 30 degrees of freedom (dof), as a result of the high-energy excess above 12 keV. The best-fit parameters in various two-component models are shown in Table 1. However, the acceptable ranges of the model parameters sensitive to the high-energy part are very large because of the poor statistics in this high-energy region. The dip spectrum does not show apparent low-energy X-ray absorption in Figure 4, which is consistent with the *EXOSAT* result. We compared the mean X-ray spectrum averaged over the dips with the spectrum outside the dips, using power law with exponential cutoff plus power law. The increase in N_H is found to be less than 9.2×10^{20} cm^{-2} at 99% confidence level, while the column density of electrons required to produce the observed mean reduction (10%) in flux during the dips by Thomson scattering is 1.5×10^{23} cm^{-2}.

The combined "low" state spectrum obtained from both *Ginga* and *ROSAT* can be fitted by various combinations of two components such as those in Table 1. However, there always exists a wavy feature in the fit residuals. In particular, a combination of the multicolor disk blackbody and a power law shows a broad line–like excess at around 7 keV such as the one shown in the top panel of Figure 5. This feature disappears when an iron emission line centered around 6.7 keV is introduced as shown in the middle and bottom panel of Figure 5. The presence of the iron line is unlikely to be an artifact of the model since various models always produce such iron lines, as shown in Table 2. The inclusion of an iron line is also justified by the *F*-test with the confidence level >99.9% for all the two-component combinations. The equivalent width is $\sim 90 \pm 37$ eV to $\sim 162 \pm 32$ eV, depending on the continuum model. The values for N_H range from $(3.7 \pm 0.2) \times 10^{21}$ to $(4.2 \pm 0.3) \times 10^{21}$ cm^{-2}, as shown in Table 2; they are somewhat smaller than the value $(5.6 \pm 0.4) \times 10^{21}$ cm^{-2} reported by White et al. (1984).

Including the reflection component in the model might be interesting to check the reality of the iron emission line, since the broad line–like features seen in some bright LMXBs have

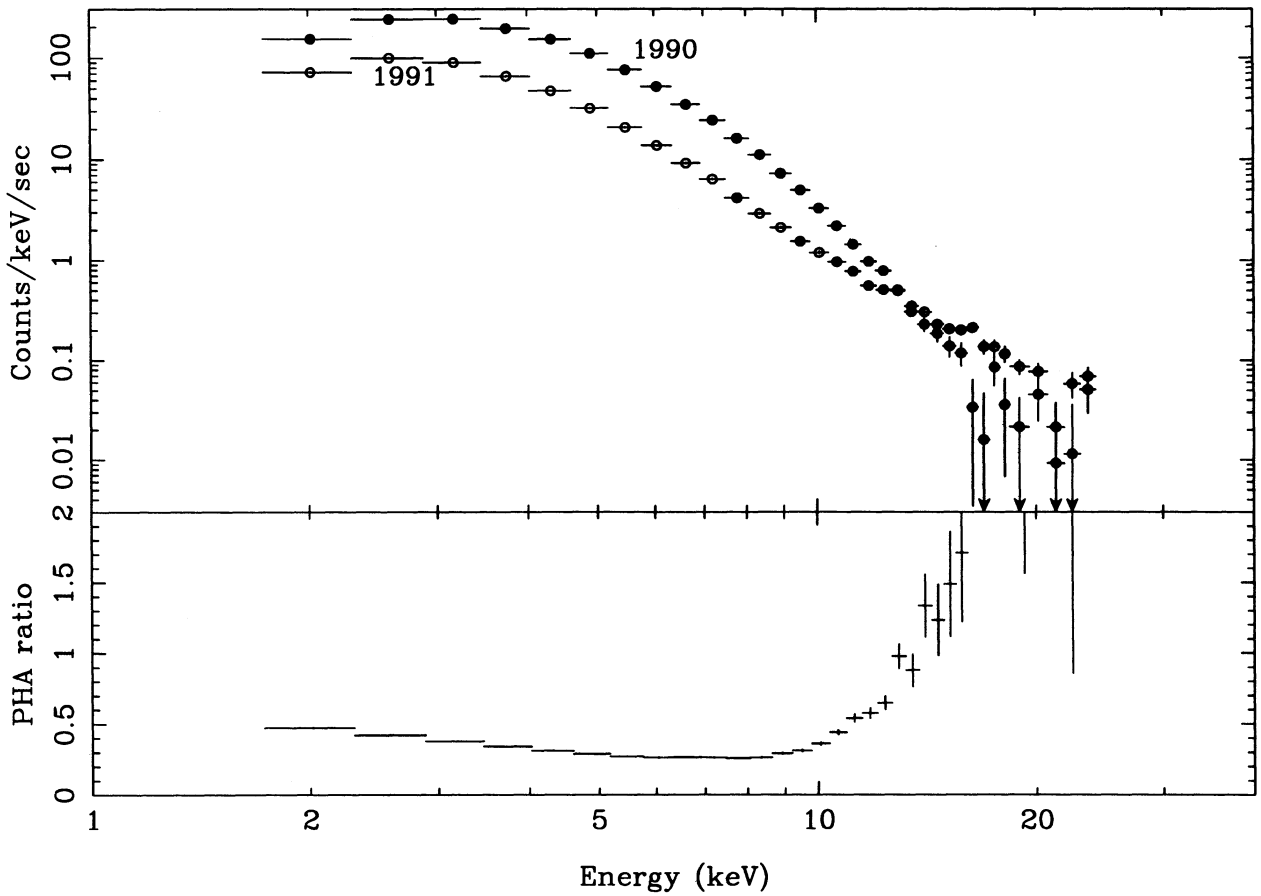

FIG. 3.—Comparison of the two spectra observed in 1990 April (high state) and 1991 September (low state). The bottom panel shows the ratio of the 1991 spectrum to the 1990 nondip spectrum.

TABLE 1

BEST-FIT PARAMETERS FOR THE 1990 OBSERVATION

Model	Spectral Parameters[a]	N_H[b] (10^{21} cm^{-2})	χ^2_ν(dof)
Multicolor disk blackbody + power law	$T_{in} = 1.24^{+0.01}_{-0.01}$ keV; $\alpha = 3.41^{+0.78}_{-0.78}$	$8.47^{+12.60}_{-4.17}$	0.43(29)
Multicolor disk blackbody + blackbody	$T_{in} = 1.24^{+0.01}_{-0.02}$ keV; $T_b = 2.60^{+0.62}_{-0.45}$ keV	$3.87^{+0.84}_{-0.79}$	0.45(29)
Multicolor disk blackbody + Comptonized blackbody[c]	$T_{in} = 1.23^{+0.02}_{-0.43}$ keV; $\alpha = 1.96^{+1.14}_{-1.34}$, $y = 0.30^{+0.34}_{-0.30}$	$4.09^{+3.28}_{-0.89}$	0.44(28)
Power law with exponential cutoff + power law	$\alpha_c < 0.13$; $E_c = 1.46^{+0.05}_{-0.02}$ keV; $\alpha = 1.91^{+1.29}_{-1.04}$	$4.13^{+2.50}_{-0.82}$	0.51(28)
Power law with exponential cutoff + blackbody	$\alpha_c < 0.13$; $E_c = 1.46^{+0.05}_{-0.01}$ keV; $T_b = 3.95^{+2.07}_{-1.02}$ keV	$3.94^{+1.52}_{-0.74}$	0.48(28)

NOTE.—Quoted errors are 90% confidence limits.

[a] T_{in} is the temperature at inner disk of the multicolor disk blackbody; α is the power-law photon index; T_b is blackbody temperature; y is the Comptonization parameter; α_c is the photon index of the exponential cutoff; E_c is the cutoff energy of the exponential cutoff.

[b] Absorption column density.

[c] The Comptonized blackbody has an assumed electron temperature $T_e = 100$ keV.

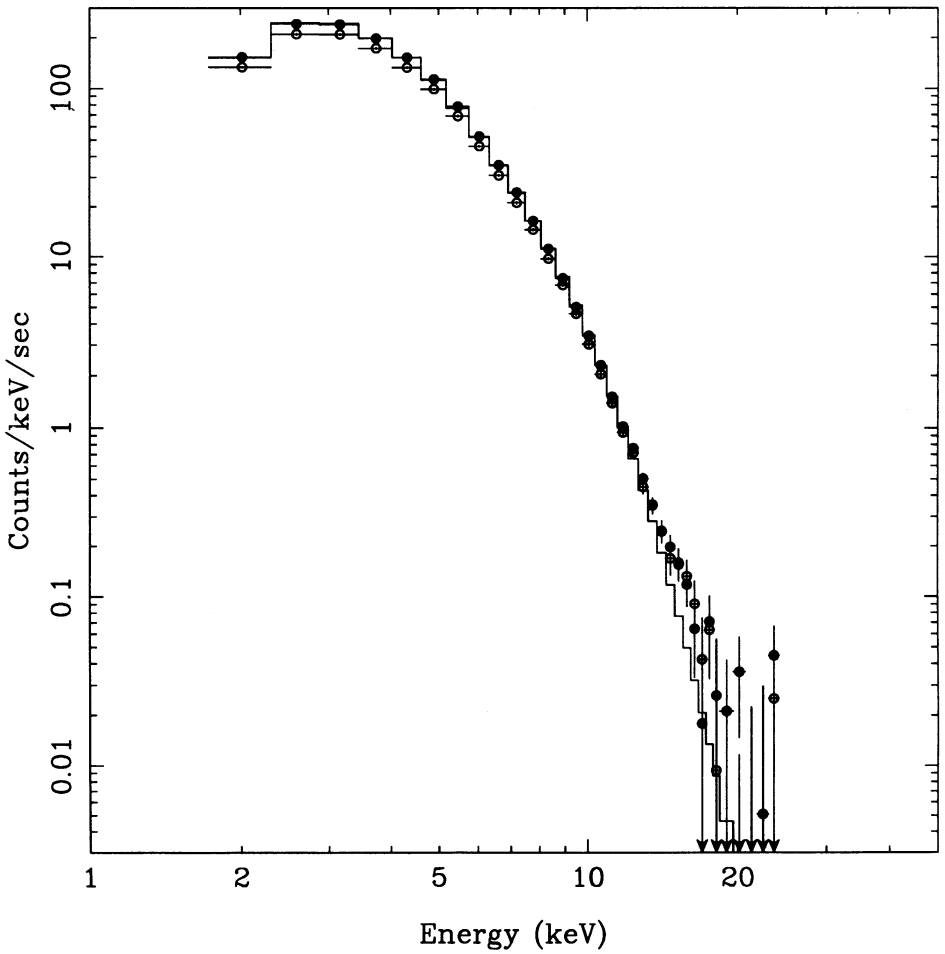

FIG. 4.—Spectra of 1755−338 obtained with *Ginga* in 1990 April. The spectrum with filled circles is obtained during the nondip intervals, while the one with open circles is for the dips. The solid line shows the best-fit power law with high-energy cutoff model to the nondip spectrum.

TABLE 2

BEST-FIT PARAMETERS FOR THE 1991 OBSERVATION

MODEL	CONTINUUM PARAMETERS[a]	IRON LINE		N_H	χ^2_ν(dof)
		E_{line} (keV)	EW (eV)	(10^{21} cm^{-2})	
Multicolor disk blackbody + power law	$T_{in} = 0.96^{+0.01}_{-0.01}$ keV; $\alpha = 2.65^{+0.10}_{-0.11}$	...	...	$4.70^{+0.30}_{-0.31}$	2.25(64)
Multicolor disk blackbody + power law + Gaussian line[b]	$T_{in} = 0.94^{+0.01}_{-0.01}$ keV; $\alpha = 2.46^{+0.13}_{-0.14}$	$6.73^{+0.13}_{-0.14}$	$162^{+26.0}_{-37.0}$	$4.21^{+0.31}_{-0.28}$	1.42(62)
Multicolor disk blackbody + Comptonized blackbody	$T_{in} = 0.64^{+0.05}_{-0.04}$ keV; $T_b = 0.90^{+0.04}_{-0.03}$ keV; $y = 0.18^{+0.02}_{-0.01}$	...	...	$3.68^{+0.14}_{-0.12}$	1.34(63)
Multicolor disk blackbody + Comptonized blackbody + Gaussian line[b]	$T_{in} = 0.63^{+0.07}_{-0.06}$ keV; $T_b = 0.86^{+0.05}_{-0.03}$ keV; $y = 0.18^{+0.03}_{-0.02}$	$6.79^{+0.18}_{-0.18}$	$106^{+39.0}_{-33.7}$	$3.67^{+0.16}_{-0.14}$	0.80(61)
Power law with exponential cutoff + power law	$\alpha_c = 0.73^{+0.11}_{-0.12}$; $E_c = 1.51^{+0.08}_{-0.07}$ keV; $\alpha = 1.49^{+0.19}_{-0.19}$	...	...	$3.96^{+0.17}_{-0.17}$	0.95(63)
Power law with exponential cutoff + power law + Gaussian line[b]	$\alpha_c = 0.60^{+0.13}_{-0.14}$ $E_c = 1.41^{+0.08}_{-0.08}$ keV; $\alpha = 1.64^{+0.19}_{-0.19}$	$6.75^{+0.19}_{-0.20}$	$90.1^{+36.9}_{-37.1}$	$3.82^{+0.18}_{-0.17}$	0.69(61)

NOTE.—Quoted errors are 90% confidence limits.

[a] T_{in} is the temperature at inner disk of the multicolor disk blackbody; α is the power-law photon index; T_b is blackbody temperature; y is the Comptonization parameter; α_c is the photon index of the exponential cutoff; E_c is the cutoff energy of the exponential cutoff.

[b] Gaussian line width (σ) is fixed at 0.1 keV; E_{line} and EW are center energy and equivalent width, respectively.

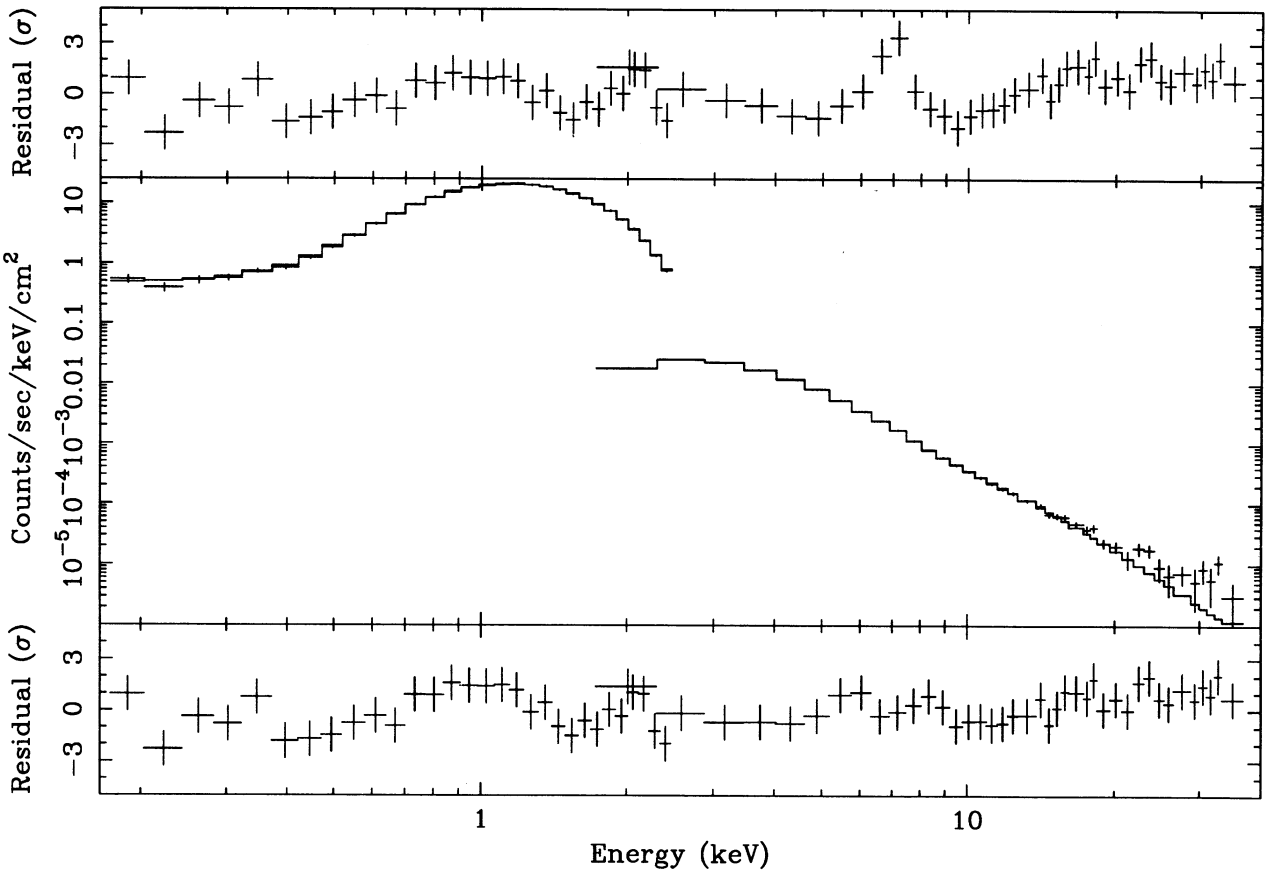

FIG. 5.—Two-component (multicolor disk blackbody and power law) fit with an iron line to the 1991 spectrum. The top panel shows a wavy feature in the 6–8 keV region in the residual when the iron line is not included, while it disappears in the bottom panel when the iron line is introduced.

been attributed to the reflection component (Mitsuda 1992). We have adopted a simple reflection model given by Lightman & White (1988), and the fitting results with the ionization state $\xi_0 = 0.02$ are shown in Table 3. In the model composed of a disk blackbody plus a power law, the covering factor is found to be rather large and the confidence level of the reality of the iron line is about 80%. However, in the other two continuum models, the existence of an iron line is essential with the confidence level above 98%.

3. DISCUSSION

We have observed 1755−338 with *Ginga* in 1990 April and simultaneously with *Ginga* and *ROSAT* in 1991 September. Analysis of the 1990 observation confirmed the recurrent dips with a period of 4.4 hr and the spectral independence of the dip events (White et al. 1984). The neutral hydrogen column density is (3.7–4.2) × 10^{21} cm^{-2} in the "low" state 1991 observation. In addition, we have the following new results:

1. A small intensity drop is observed about halfway between the two primary dips just after April 25, 20 UT in 1990. It is not certain if it actually is a dip, but it should be noted that "anomalous" dips were observed previously in other LMXB sources such as 1916−053 (Smale et al. 1988) and Her X-1 (Voges et al. 1985). There are at least two mechanisms suggested which could produce the secondary dip. Lubow (1989) argued that the gas stream at several scale heights above the plane of the binary orbit is able to flow over the disk once it passes the disk edge. In this model, the second dip could be the result of the final impact of relatively high, free-flowing gas onto the disk. Alternatively, the tidal forces caused by the companion star may cause the matter on the rim of the disk, presumably at some selected phases, to be pulled out of the orbital

TABLE 3

APPLICATION OF THE REFLECTION MODEL

Model	E_{line} (keV)	EW (eV)	Covering Factor	χ^2_ν (dof)	P^a (%)
Multicolor disk blackbody + power law + Gaussian line	$6.63^{+0.41}_{-0.43}$	$44.1^{+39.8}_{-40.7}$	$0.63^{+0.05}_{-0.11}$	0.96(61)	80.2
Power law with exponential cutoff + power law + Gaussian line	$6.75^{+0.19}_{-0.20}$	$90.1^{+36.9}_{-39.0}$	<0.34	0.70(60)	99.8
Multicolor disk blackbody + Comptonized blackbody + Gaussian line.....	$6.77^{+0.23}_{-0.27}$	$72.9^{+47.6}_{-45.0}$	$0.23^{+0.19}_{>0.}$	0.77(60)	98.4

NOTE.—Quoted errors are 90% confidence limits.

[a] Confidence level of the reality of the iron line, when the reflection component is included.

plane (Pandey 1989). The material pulled out of the orbital plane between $\phi = 0.2$, $\phi = 0.3$ and $\phi = 0.7$, $\phi = 0.8$ (with mid-eclipse as the zero phase) could cause the secondary and the primary dips, respectively.

2. A "low" intensity state with the flux less than 35% of the "high" state "nondip" level is observed in 1991. A folded light curve shows that the dips are even shallower than those of the "high" state. Parmar et al. (1986) found that the dip strength in the X-ray light curve of 0748−676 was generally greater during periods of higher X-ray luminosity. The present observation confirms this dependence of the dip activity on the X-ray intensity. The low X-ray intensity likely reflects reduced mass transfer, which may cause a reduction of the size of the obscuring region. This is consistent with the idea that the origin of the dips lies in the accretion flow.

3. The spectrum in the "low" state (1991) is hard compared to that in the "high" state (1990). The black hole candidates and some LMXBs generally change their state from the soft state to the hard state when the luminosity decreases.

4. An iron emission line centered around 6.7 keV is observed in the "low" state (1991). The equivalent width ranges from $\sim 90 \pm 37$ eV to $\sim 162 \pm 32$ eV (90% confidence) depending on the assumed continuum model. The detected equivalent width is similar to those in other LMXBs, which suggests that the metallicity of 1755−338 is not much different from other sources (White et al. 1986). Although the equivalent widths become somewhat smaller when the reflection component is included, the reality of the iron emission is justified with the confident level above 98% by the F-test in two continuum models; while the third model (disk blackbody plus a power law) gives a rather large covering factor, and the confidence level of the reality of the iron line is about 80% in this case.

Since a significant iron line seems to be present in the "low" state spectrum, it is interesting to see if the similar line feature could also be identified in the "high" state spectrum. Table 4 shows 90% confidence upper limits on the iron line flux during the nondip and dip states. As the upper limit of the line flux in the "high" state nondip spectrum is larger than, or within the error range of, the flux of the "low" state iron line, it is possible that the iron line flux remains unchanged and the line feature is masked by the continuum in the "high" state. The equivalent width is significantly lower in the "high" state, which implies that the iron line intensity does not increase as much as the continuum flux. In some LMXBs (for example, Sco X-1 during the flaring states; White, Peacock, & Taylor 1985; see also Hirano et al. 1987) it has been observed that the iron line intensities remain more or less the same. The upper limit of the line flux obtained from the "high" state dip spectrum is smaller than the line flux observed during the "low" state. If we assume that the line intensity is unchanged, the reduction must come from the blocking of the emission region of the iron line. This line emission region is probably relatively close to the central source, since the energy of the line center is 6.7 keV, which is higher than 6.4 keV of the usual fluorescence line emitted from the neutral iron at the cooler outer region. The equivalent width also decreases in the "dip" state. If the dip is caused by the blocking material, such a reduction in the equivalent width implies that the line-emitting region is more blocked than the continuum-emitting region.

The source 1755−338 has received special attention because of the spectral independence of its dip spectrum. This led White et al. (1984) to suggest that the absorbing medium in the system is severely underabundant in heavy elements. The dips found in the light curve of the globular cluster X-ray source 1746−371 are similar to those observed from 1755−338 in that the spectra are energy independent and the dips are shallow (Parmar, Stella, & Giommi 1989). There is some evidence that the 1746−371 system is not an accretion disk corona source and that the overall heavy-element abundance of NGC 6441 is only a factor of 4–10 less than that of the solar abundance (Sztajno et al. 1987; Pilachowski 1984). Parmar et al. (1989) argued that completely photoionized obscuring material and two (or more) emission regions could account for energy-independent variations of 1746−371. Frank & Sztajno (1984) suggested another possibility regarding 1755−338, i.e., that the energy independence of the dips results from the partial occultation of an extended X-ray source similar to that seen in the accretion disk coronae sources. However, Parmar et al. (1985) pointed out that the source is an LMXB with $L_x/L_{opt} \sim 10^3$ (i.e., much larger than for an ADC source), which implies that the central source is directly seen rather than as scattered emission, as is the case for the other partial eclipsing sources. Obscuration by a fully ionized medium is also unlikely, since the outer edge of the accretion disk cannot be fully ionized (Parmar et al. 1985). Our finding of an iron emission line at a strength similar to that in other LMXBs makes the possibility of the absorption by extremely underabundant material unlikely.

Frank, King, & Lasota (1987) made a physical model for the light curves of low-mass X-ray binaries and pointed out that if a two-component spectrum is assumed, it is possible to arrange the relative fluxes of these two components in such a way that very little hardening occurs for shallow dips. Church & Bałucinska (1993) adopted this idea and analyzed the *EXOSAT* data using a two-component model consisting of a

TABLE 4

COMPARISON OF IRON LINE BETWEEN LOW STATE AND HIGH STATE

			High State (1990)[a]			
	Low State (1991)		Nondip		Dip	
Model	EW[b]	F_{line}[c]	EW[b]	F_{line}[c]	EW[b]	F_{line}[c]
Multicolor disk blackbody + power law + Gaussian line	$162^{+26.0}_{-37.0}$	$3.08^{+0.70}_{-0.68}$	<33.8	<2.73	<8.59	<0.62
Multicolor disk blackbody + Comptonized blackbody + Gaussian line	$106^{+39.0}_{-33.7}$	$2.05^{+0.74}_{-0.71}$	<32.6	<2.63	<11.0	<0.79
Power law with exponential cutoff + power law + Gaussian line	$90.1^{+36.9}_{-37.1}$	$1.78^{+0.71}_{-0.72}$	<36.0	<2.88	<11.6	<0.83

NOTE.—Quoted errors are 90% confidence limits.

[a] Line center energy is fixed at 6.7 keV.

[b] Equivalent width of an iron line, in units of eV.

[c] Line flux of an iron line, in units of 10^{-4} photons cm^{-2} s^{-1}.

TABLE 5

SPATIALLY SEPARATED TWO-COMPONENT MODEL

MODEL	NONDIP		DIP	
	F_{soft}[a]	F_{hard}[b]	R[c]	ΔN_H[d]
Cutoff + power law.....	$19.83^{+2.11}_{-0.57}$	$0.50^{+1.62}_{-0.19}$	$0.91^{+0.01}_{-0.01}$	$28.10^{+24.36}_{-27.60}$
Cutoff + blackbody.....	$20.07^{+2.21}_{-0.61}$	$0.22^{+0.09}_{-0.04}$	$0.90^{+0.01}_{-0.01}$	$20.28^{+25.96}_{>0.}$

NOTE.—Quoted errors are 90% confidence limits.

[a] Flux in the soft component in units of 10^{-10} ergs cm^{-2} s^{-1}.

[b] Flux in the hard component in units of 10^{-10} ergs cm^{-2} s^{-1}.

[c] Reduction factor of the normalization for soft component compared with the best-fit parameter of nondip spectrum.

[d] Increase of the absorption column density of hard component during the dip, in units of 10^{22} cm^{-2}.

blackbody plus a power law, each component having its own cosmic abundance absorption term. They obtained a high value of N_H, $\sim 10^{22}$ cm^{-2}, for the blackbody component. Also, energy-independent dipping is seen to be caused by an increase in N_H for the blackbody component which dominates in the energy range between 3 keV and 6 keV, while N_H for the power-law component which is dominant for energies smaller than 1.5 keV or larger than 8 keV increases only slightly. We tried the same model, blackbody plus a power law, to fit the "high" state nondip spectrum. We obtained a good χ^2_ν value 1.06 for 29 dof, but N_H, this time for the power-law component, is around 3.48×10^{22} cm^{-2}, which is an order of magnitude higher than the values obtained from the other models in Table 1. Such a high value of N_H is not consistent with the results obtained from the H I survey (Stark et al. 1992). We proceed with our own models shown in Table 1 to test the idea of different absorption in the two components. The hard components of the models in Table 1, which should yield a large increase in N_H during the dip for the idea of Frank et al. (1987) to work in the present analysis, generally have large uncertainties in their fluxes because of the poor statistics in the high-energy region, as two examples show in Table 5. Nevertheless, we adopted these models and tried to fit the dip spectrum in the following form using the value of A_s and A_h, which are the normalizations for the model spectrum f_s of the soft component and for f_h of the hard component, respectively, determined from the nondip spectrum

$$e^{-\sigma N_H}(RA_s f_s + e^{-\sigma \Delta N_H} A_h f_h) .$$

Here R represents the reduction of the soft component flux and ΔN_H is the increase in the absorption column density for the hard component. The above model implicitly assumes that the soft component comes from an extended source which is partially blocked during the dip and that the hard component emitted from the central source is absorbed by the blocking material. The fit results are shown in the right two columns in Table 5. The soft component is blocked about 10% during the dip. The absorption column density for the hard component varies according to the model and is not well determined, as the large error range indicates. The uncertainty in ΔN_H mainly comes from the poor statistics in the high-energy region. Nevertheless, there is a certain indication that ΔN_H for the hard component increases by an order of magnitude, which is consistent with the idea of Frank et al. (1987). In this regard, the dips of 1755−338 may result from the partial obscuration of an extended source, while the emission from the central source is heavily absorbed. This picture is consistent with the idea that the iron lines originate from the region relatively close to the central source, since the equivalent width of the iron line also decreases during the dip. However, the χ^2_ν value in these fits is around 1.6 with 32 dof, which is not good enough to draw a definite conclusion, and we still cannot exclude the possibility of the obscuration of the central source by the overflowing stream if it is very close to the central source and significantly photoionized.

An interesting feature of 1755−338 is its ultrasoft spectrum. White & Marshall (1984) pointed out that such soft X-ray spectra may be a signature of "high" state accreting black hole candidates. Some black hole candidates exhibit typical bimodal spectral behavior, "high" state being soft, while the "low" state spectrum is hard. The "high" state spectrum consists of an ultrasoft component and a hard tail, whereas the "low" state is best represented by a hard power-law spectrum (for a review, see Tanaka & Lewin 1995). The source 1755−338 observed in the present study does show spectral changes. However, the behavior is not as distinct as that of the black hole candidates GX 339-4 and Cyg X-1, and among the neutron stars there also exists the tendency for the spectra to become harder at lower luminosities (van der Klis 1994; van Paradijs & van der Klis 1994).

The multicolor disk blackbody model has been quite successful in describing the soft component of the LMXBs and the black hole candidates. Also, it has been pointed out that the values for $r_{in}(\cos\theta)^{1/2}$, where r_{in} is the inner radius of the disk and θ is the inclination of the disk, are more or less constant regardless of the spectral states for the known black hole

TABLE 6

FIT PARAMETERS OF MULTICOLOR DISK BLACKBODY AND FLUXES

Model	Data	$r_{in}(\cos\theta)^{1/2}$[a]	T_{in} (keV)	F_{soft}[b]	F_{hard}[c]
Multicolor disk blackbody + power law	G90[d]	$2.22^{+0.55}_{-0.11}$	$1.24^{+0.01}_{-0.01}$	16.78	3.88
Multicolor disk blackbody + power law + Gaussian line	G91[e]	$2.00^{+0.09}_{-0.04}$	$1.00^{+0.01}_{-0.02}$	7.23	2.00
	GR91[f]	$2.30^{+0.05}_{-0.05}$	$0.94^{+0.01}_{-0.01}$	5.84	2.53
Multicolor disk blackbody + Comptonized blackbody	G90	$2.32^{+2.47}_{-0.10}$	$1.23^{+0.02}_{-0.43}$	20.16	0.58
Multicolor disk blackbody + Comptonized blackbody + Gaussian line.....	G91	$2.28^{+0.58}_{-0.16}$	$0.96^{+0.03}_{-0.15}$	7.65	1.55
	GR91	$5.04^{+0.99}_{-0.90}$	$0.63^{+0.07}_{-0.06}$	3.89	4.69

NOTE.—Quoted errors are 90% confidence limits.

[a] r_{in} and θ are the inner radius and the angle of disk, respectively, for an assumed distance of 3 kpc.

[b] Bolometric flux in the soft component in units of 10^{-10} ergs cm^{-2} s^{-1}.

[c] Bolometric flux in the hard component in units of 10^{-10} ergs cm^{-2} s^{-1}.

[d] Data obtained from *Ginga* in 1990.

[e] Data obtained from *Ginga* in 1991.

[f] Combined data with *Ginga* and *ROSAT* in 1991.

candidates, while they are variable for LMXBs containing neutron stars (Tanaka 1989; Ebisawa et al. 1992). The results of $r_{in}(\cos\theta)^{1/2}$ and T_{in}, the temperature at the inner radius, for 1755−338 deduced from the present study are listed in Table 6. When the power-law model is adopted as a hard component, the values are nearly constant regardless of the spectral states. This may support the idea that the compact object in the source is a black hole. However, the derived values of $r_{in}(\cos\theta)^{1/2}$ for 1755−338 are $\sim$2.2 km at an assumed distance of 3 kpc, while the values for the black hole candidates are typically 20–30 km (Tanaka 1989; Yaqoob, Ebisawa, & Mitsuda 1993). These values obtained for 1755−338 are rather close to the values for LMXBs, even if we take into account the uncertainties in the distance to the source and in the inclination angle of the system relative to the observer. When the Comptonized blackbody model is used for a hard component, the *Ginga* data alone again show more or less the constant results for $r_{in}(\cos\theta)^{1/2}$ on the one hand, while the combined data from *Ginga* and *ROSAT* yield quite different fitting results, on the other hand. It seems that the present study does not give conclusive tips as to the nature of the central source, and we need more study to identify whether 1755−338 is a black hole or not.

M. v. d. K. acknowledges support from the Netherlands Organization for Scientific Research (NWO) under grant PGS 78-277. W. H. G. L. acknowledges support from the National Aeronautics and Space Administration under grant NAG8-216.

REFERENCES

Bradt, H., & McClintock, J. E. 1983, ARA&A, 21, 13
Church, M. J., & Bałucinska, M. 1993, MNRAS, 260, 59
Cominsky, L. C., & Wood, K. 1984, ApJ, 283, 765
Ebisawa, K., Makino, F., Mitsuda, K., Belloni, T., Cowley, A. P., Schmidtke, P. C., & Treves, A. 1992, in Frontiers of X-Ray Astronomy, ed. Y. Tanaka & K. Koyama (Tokyo: Universal Academy Press), 351
Frank, J., King, A. R., & Lasota, J.-P. 1987, A&A, 178, 137
Frank, J., & Sztajno, M. 1984, A&A, 138, L15
Hirano, T., Hayakawa, S., Nagase, F., Masai, K., & Mitsuda, K. 1987, PASJ, 39, 619
Jones, C. 1977, ApJ, 214, 856
Lightman, A. P., & White, T. R. 1988, ApJ, 335, 57
Lubow, S. H. 1989, ApJ, 340, 1064
Makino, F., & the ASTRO-C team 1987, Astrophys. Lett. Commun., 25, 223
Mason, K. O. 1986, in Lecture Notes in Physics, Vol. 266, The Physics of Accretion onto Compact Objects, ed. K. O. Mason, M. G. Watson, & N. E. White (Berlin: Springer), 113
———. 1989, in Proc. 23rd ESLAB Symposium, Two Topics in X-Ray Astronomy, ed. J. Hunt & B. Battrick (ESA SP-296), 113
Mason, K. O., Parmar, A. N., & White, N. E. 1985, MNRAS, 216, 1033
McClintock, J. E., Canizares, C. R., & Hiltner, W. A. 1978, IAU Circ., No. 3251
Mitsuda, K. 1992, in Frontiers of X-Ray Astronomy, ed. K. Koyama & H. Kunieda (Tokyo: Universal Academy Press), 115
Pandey, U. S. 1989, A&A, 221, 62
Parmar, A. N., Stella, L., & Giommi, P. 1989, A&A, 222, 96
Parmar, A. N., & White, N. E. 1988, Mem. Soc. Astron. Italiana, 59, 147
Parmar, A. N., White, N. E., Giommi, P., & Gottwald, M. 1986, ApJ, 308, 199
Parmar, A. N., White, N. E., Sztajno, M., & Mason, K. O. 1985, Space Sci. Rev., 40, 213
Pilachowski, C. A. 1984, ApJ, 281, 614
Smale, A. P., Mason, K. O., White, N. E., & Gottwald, M. 1988, MNRAS, 232, 647
Stark, A. A., Gammie, C. F., Wilson, R. W., Bally, J., Linke, R. A., Heiles, C., & Hurwitz, M. 1992, ApJS, 79, 77
Stella, L., Priedhorsky, W., & White, N. E. 1987, ApJ, 312, L17
Sztajno, M., Fujimoto, M. Y., van Paradijs, J., Vacca, W. D., Lewin, W. H. G., Pennix, W., & Trümper, J. 1987, MNRAS, 226, 39
Tanaka, Y. 1989, in Proc. 23rd ESLAB Symposium, Two Topics in X-Ray Astronomy, ed. J. Hunt & B. Battrick (ESA SP-296), 3
Tanaka, Y., & Lewin, W. H. G. 1995, in X-Ray Binaries, ed. W. H. G. Lewin, J. van Paradijs, & E. P. J. van der Heuvel (Cambridge: Cambridge Univ. Press), in press
Trümper, J. 1983, Adv. Space Res., 2 (4), 241
Turner, M. J. L., et al. 1989, PASJ, 41, 345
van der Klis, M. 1994, ApJS, 92, 511
van Paradijs, J. 1995, in X-Ray Binaries, ed. W. H. G. Lewin, J. van Paradijs, & E. P. J. van der Heuvel (Cambridge: Cambridge Univ. Press), in press
van Paradijs, J., & van der Klis, M. 1994, A&A, 281, L17
Voges, W., Kahabka, H., Ögelman, H., Pietsch, W., & Trümper, J. 1985, Space Sci. Rev., 40, 339
Vrtilek, S. D., Kahn, S. M., Grindlay, J. E., Helfand, D. J., & Seward, F. D. 1986, ApJ, 307, 698
White, N. E., & Marshall, F. E. 1984, ApJ, 281, 354
White, N. E., & Mason, K. O. 1985, Space Sci. Rev., 40, 167
White, N. E., Nagase, F., & Parmar, A. N. 1995, in X-Ray Binaries, ed. W. H. G. Lewin, J. van Paradijs, & E. P. J. van der Heuvel (Cambridge: Cambridge Univ. Press), in press
White, N. E., Parmar, A. N., Sztajno, M., Zimmermann, H. U., Mason, K. O., & Kahn, S. 1984, ApJ, 283, L9
White, N. E., Peacock, A., Hasinger, G., Mason, K. O., Manzo, G., Taylor, B. G., & Branduardi-Raymont, G. 1986, MNRAS, 218, 129
White, N. E., Peacock, A., & Taylor, B. G. 1985, ApJ, 296, 475
White, N. E., & Swank, J. H. 1982, ApJ, 253, L61
Yaqoob, T., Ebisawa, K., & Mitsuda, K. 1993, MNRAS, 264, 411